Applied Catalysis B: Environmental 240 (2019) 1–8

Contents lists available at ScienceDirect

Applied Catalysis B: Environmental

journal homepage: www.elsevier.com/locate/apcatb

Copper oxide nanowires for efficient photoelectrochemical water splitting

Jianming Li[a,1], Xu Jin[a,1], Rengui Li[b,*], Yue Zhao[b], Xiaoqi Wang[a], Xiaodan Liu[a], Hang Jiao[a]

[a] Research Institute of Petroleum Exploration & Development (RIPED), PetroChina, No. 20 Xueyuan Road, Haidian District, Beijing, 100083, PR China
[b] State Key Laboratory of Catalysis, Dalian Institute of Chemical Physics, Chinese Academy of Sciences, Dalian National Laboratory for Clean Energy, The Collaborative Innovation Center of Chemistry for Energy Materials (iChem-2011), Zhongshan Road 457, Dalian, 116023, PR China

ARTICLE INFO

Keywords:
Photoelectrochemical
Hydrogen production
CuO
Nanowire

ABSTRACT

Photoelectrochemical (PEC) splitting of water into hydrogen and oxygen by the direct use of sunlight is an ideal, renewable method for solar-to-chemical conversion. Photocathodes based on p-type copper oxide (CuO) are promising materials for large-scale and widespread PEC water splitting due to the abundance of copper element, suitable band gap, and favorable band alignments. In this work, we fabricated one-dimensional CuO nanowires on Cu foils via a facile thermal-treatment process for PEC water splitting. The well-defined CuO nanowire-based photocathodes exhibit an obvious photocurrent responsive character of a p-type semiconductor with onset potential at ~700 mV vs. RHE. The CuO photocathode shows a photocurrent of ~1.4 mA cm^{-2} at 0 V vs. RHE under AM 1.5 G irradiation, which is one of the highest photocurrents based on bare CuO photocathode. Further depositing Pt nanoparticles as cocatalyst on the surface of CuO nanowires to accelerate surface reaction and inhibit charge accumulating at semiconductor/solution interface, resulting in a significant improvement of the stability for photoelectrodes. Our work reports a promising method for fabricating well-defined metal oxides-based photoelectrodes, which providing a promising candidate for highly efficient no bias PEC devices for solar fuels production.

1. Introduction

Artificial photosynthesis for chemicalfuels production using solar energy is one of attractive and sustainable solutions for solving energy and environmental problems [1–4]. Photoelectrochemical (PEC) splitting of water into hydrogen and oxygen by the direct use of sunlight is an ideal, renewable method of hydrogen production that integrates solar energy collection and water electrolysis into a single photoelectrode [5–9]. A photoelectrochemical water splitting cell is based on a semiconductor/solution junction, where the minority charges (electrons for a p-type semiconductor and holes for an n-type semiconductor) generated upon photoexcitation in the semiconductor are driven into the solution by the electric field at the junction, where they can drive a redox reaction, such as the reduction of protons to H_2 for a p-type semiconductor [10]. For PEC water splitting, most of the researches focusing on investigation of n-type photoanodes (e.g., $BiVO_4$, Ta_3N_5, Fe_2O_3), on which water oxidation takes place while protons are reduced to hydrogen at the counter electrodes. However, when constructing an integrated no-bias PEC system, both photocathodes and photoanodes are required. Photoanodes in PEC water splitting usually suffer from significant photo-corrosion due to the self-oxidation at the semiconductor/liquid junction by the photo-excited holes [11]. Furthermore, owing to the low density of solar energy and requirement for widespread solar energy harvesting, the photoelectrodes use in PEC device must be low-cost and fabricated from earth-abundant elements using scalable processing techniques [12]. Binary copper semiconductors, such as copper oxides (Cu_2O, CuO), are a class of attractive materials because they are photoactive, earth-abundant and the materials can be processed by industrially proven and low-cost methods [10]. CuO is a p-type semiconductor with a narrow band gap (~1.2 eV), which possesses a monoclinic crystal structure [13–15]. It has reported that the CuO electrodes made by flame spray pyrolysis of nanoparticles on FTO substrates or fast annealing under H_2/O_2 flame under temperature of more than 1000 °C can be used as photocathodes for PEC water splitting [16–18]. However, the reported photocurrents for CuO photoelectrodes are still low enough, which may be possibly due to the poor charge separation and transferring properties among semiconductor nanoparticles and also from nanoparticles to conducting substrates.

One-dimensional structured semiconductors, such as nanorods and nanowires, exhibit unique photoelectric properties, especially for the charge transportation, which have become important building blocks of

* Corresponding author.
E-mail address: rgli@dicp.ac.cn (R. Li).
[1] Both authors contribute equally to this work.

https://doi.org/10.1016/j.apcatb.2018.08.070
Received 2 June 2018; Received in revised form 2 August 2018; Accepted 27 August 2018
Available online 29 August 2018
0926-3373/

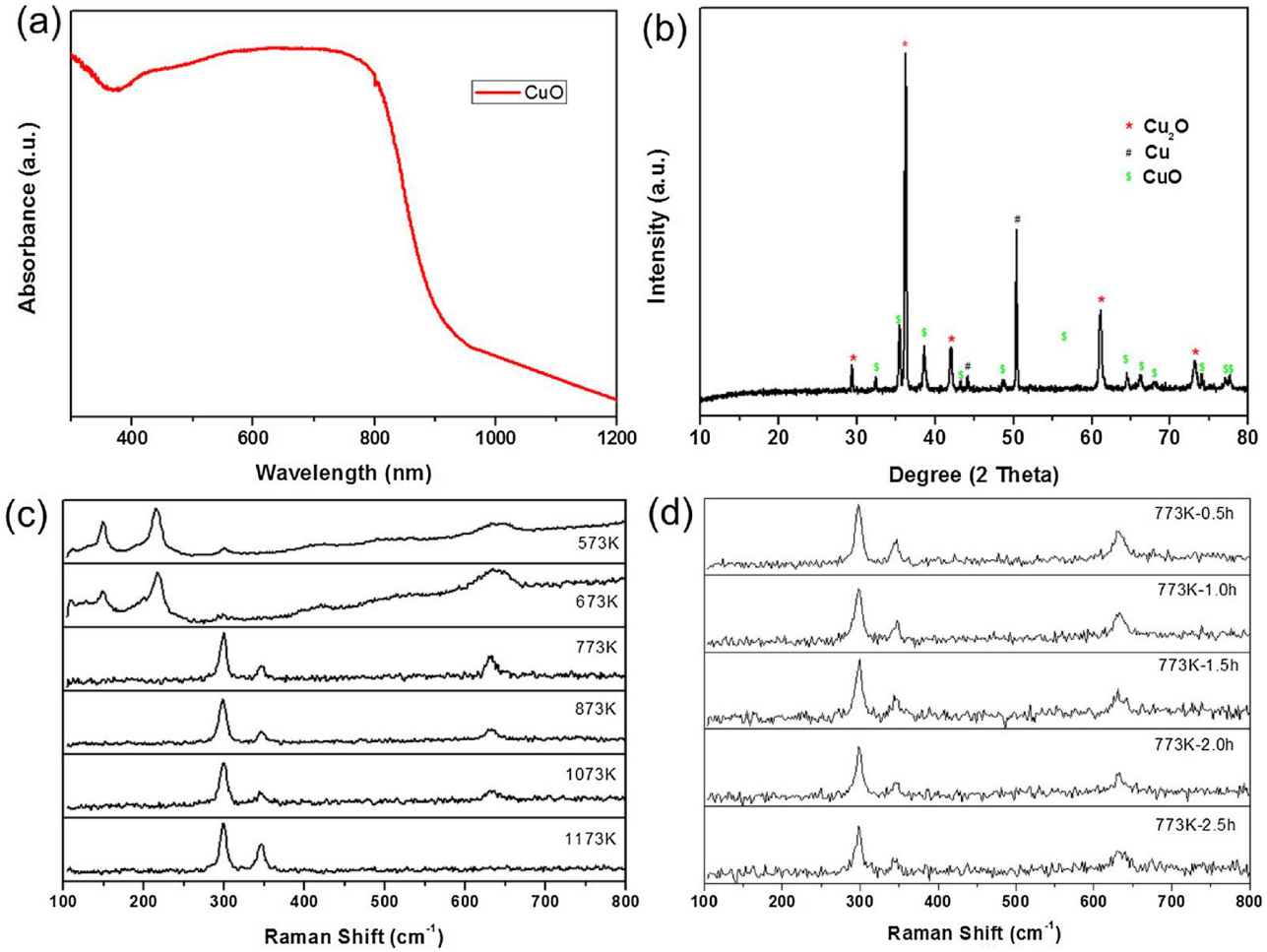

Fig. 1. Characterizations of as-prepared photocathodes via thermal-treating of Cu foils. (a) UV–vis diffusion spectra, (b) XRD patterns and (c, d) Raman shifts of photocathodes prepared under different temperatures.

nano-devices and integrated nano-systems in catalysis and energy related field [19–22]. In this work, we fabricated CuO nanowires on Cu foil as substrates via a simple thermal treatment process for PEC water splitting. The well-defined CuO nanowire photoelectrodes exhibit an obvious photocurrent responsive character of a p-type semiconductor with onset potential at ~700 mV vs. RHE. The optimized CuO photocathode shows a photocurrent of ~1.4 mA cm^{-2} at 0 V vs. RHE under AM 1.5 G irradiation, which is one of the best photocurrent based on bare CuO photocathode for PEC water splitting. Further depositing Pt nanoparticles as cocatalyst on the surface of CuO nanowires to inhibit the charge accumulating at semiconductor/solution interface, resulting in a significant improvement of the stability for photoelectrodes.

2. Experimental section

2.1. Electrodes preparation

Commercial Cu foils with 0.1 mm (purity: 99.9% Cu) thickness are used in the experiment. Cu foils are first washed in an aqueous solution of 1.5 M HCl for 5 min, rinsed in deionized water, and then dried at 60 °C before oxidized. The Cu foils was cut to the fixed area of 2 cm^2 (1 cm × 2 cm), and vertically placed in quartz crucible, and put in a muffle furnace for thermal treatment under different temperatures (300 °C–800 °C) for different times under the atmosphere of air. Pt cocatalyst was deposited on as-prepared CuO electrodes by electrochemical deposition in a three-electrode system, the applied bias is −0.5 V and the deposition time is varied from 15 s to 300 s.

2.2. Characterization of catalysts

The as-prepared samples were characterized by X-ray powder diffraction (XRD) on a Rigaku D/Max-2500/PC powder diffractometer. The sample powder was scanned using Cu-Kα radiation with an operating voltage of 40 kV and current of 200 mA. The scan rate of 5°/min was applied to record the patterns in the range of 10–80° at a step size of 0.02°. UV–vis (UV–vis) diffuse reflectance spectra were recorded on a UV–vis spectrophotometer (JASCO V-650) equipped with an integrating sphere. The morphologies of electrodes prepared under different temperatures were examined by scanning electron microscopy (SEM) taken with a Quanta 200 FEG scanning electron microscope. HRTEM micrographs were taken on a FEI Tecnai G^2 F30 transmission electron microscope.

2.3. Photoelectrochemical measurements

The photoelectrochemical performance of the electrodes was evaluated in a three-electrode configuration under front-side simulated AM1.5 illumination using an potentiostat (Iviumstat, Ivium Technologies) (100 mW cm^{-2}, Newport Sol 3 A, Class AAA Solar simulator). The fabricated electrode, a platinum electrode, and saturated calomel electrode (SCE) were used as working, counter and reference electrodes, respectively. The electrolyte was a 1.0 M Na_2SO_4 solution. The scan rate for the linear sweep voltammetry and for the cyclic voltammetry was 30 mVs^{-1}. All measured potentials were converted to V vs. RHE ($E_{RHE} = E_{SCE} + 0.244 + 0.059 \times pH$). Photocurrent stability

tests were carried out by measuring the photocurrent produced under chopped light irradiation (light/dark cycles of 30 s) at a fixed electrode potential of 0 V vs. RHE.

3. Results and discussion

CuO nanowires were prepared using a thermal-treatment method under different temperatures in the atmosphere of air using commercial Cu foil as precursor similar to the reported work [19]. Both one-step and two-step thermal-treatment processes are introduced for comparison. One-step thermal-treatment means Cu foil was directly calcinated under the required temperature for different times (denoted as CuO-T, T is calcination temperature). For the two-step thermal-treatment process, the calcination of Cu foil was controlled by a temperature programmed process, that is, Cu foil was first calcinated under low temperature (T1, < 400 °C) and then switched to a high temperature region (T2, 500–800 °C) for different times. In our experiment, all the samples were first treated under 300 °C, and then varied the post-treatment temperature in the range of 500 °C–800 °C. The obtained samples was denoted CuO-T1-T2.

Both samples prepared by one-step and two-step calcinations apparently appear black gray color and their light absorption ranges can reach more than 900 nm with an absorption tail expands to nearly 1200 nm (Fig. 1a), corresponding to an band gap of ~1.0–1.3 eV. The light absorption properties are more similar to the characteristic of CuO species as the intrinsic band gaps of CuO and Cu_2O are ~1.2 eV and 2.1 eV, respectively [23–25]. The prepared electrodes are also characterized by X-ray diffraction (Fig. 2b). It can be seen that two copper oxide phases, CuO and Cu_2O, and a pure Cu phase were detected, indicating that the oxidized sample was composed of CuO, Cu_2O, and Cu. All the three phases appeared after calcination under temperatures in the range of 300 °C to 700 °C. The XRD results show that the diffraction peaks corresponding to Cu_2O and CuO phases are oxidation products generated on Cu substrates, forming an electrode in accordance with the order of CuO, Cu_2O and Cu species from outer to inner layer. When the calcination temperatures are higher than 700 °C, only the CuO phase without Cu_2O and Cu species can be observed. The phase transformation during the thermal treatment process was also collected by XRD characterizations for photoelectrodes calcinated under different temperatures (Fig. S1). It can be clearly observed that the diffraction peaks of Cu_2O increase gradually when the temperatures ranging from 300 °C to 500 °C, and then decline when further increasing the temperature. However, the diffraction peaks of CuO increase remarkably along with the decreasing of Cu_2O peaks, when the temperature is higher than 700 °C, the main phase of photoelectrode is CuO phase. The result evidently implies the phase transformation from Cu_2O to CuO during the thermal treatment process. Raman shifts of the electrodes also confirm the XRD results, when the temperatures are lower than 400 °C, the main products on the surface is Cu_2O, which can be further oxidized to CuO species by increasing the calcination temperature, indicating temperature is a dominant factor in phase variation of oxidation products (Fig. 1c and d).

Fig. 2 shows the SEM images of the electrodes after thermal treatment of Cu foil under different temperatures. It can be found that well-defined arrays with wire-like morphologies are formed on the substrates. The nanowires formed at 500 °C reveal a high density and regular morphology with lengths ranging from 5 to 20 μm and diameters varying from 50 to 100 nm. The obtained CuO nanowires exhibit well-defined morphologies and good crystallinity. Further increasing the calcination temperature to 600 °C, the morphology of CuO nanowires becomes more uniform and straight, while the diameter was slightly reduced. It should be noted that the temperature lower than 400 °C cannot induce the formation of CuO nanowires, but produce a thin layer of Cu_2O species on the surface. When the temperature was

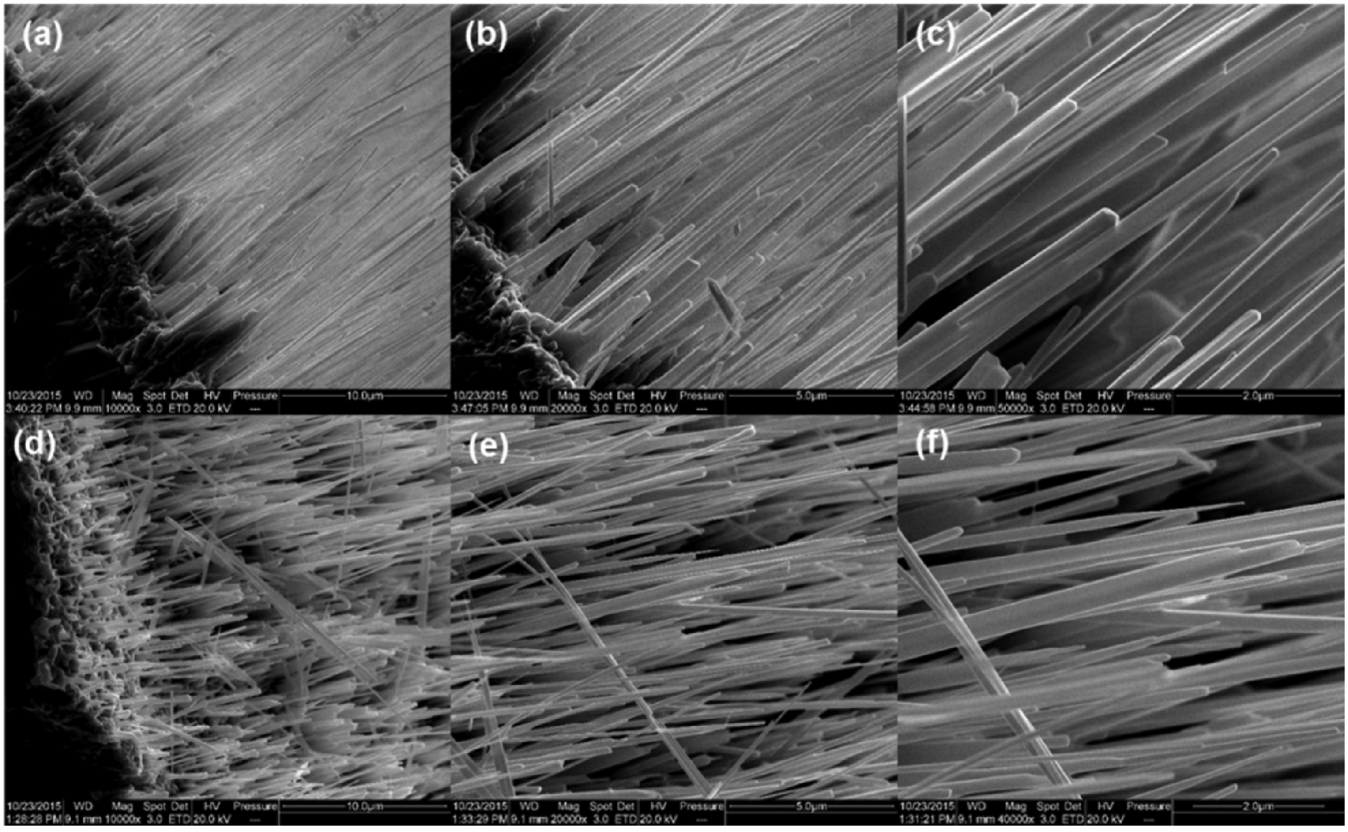

Fig. 2. SEM images of CuO nanowires treated under different conditions. (a, b, c) CuO-300-500, and (c, d, e) CuO-300-600. CuO-300-500 means CuO nanowire was prepared by thermal treatment at 300 °C for 2 hs first and then at 500 °C for 2 hs via temperature program process.

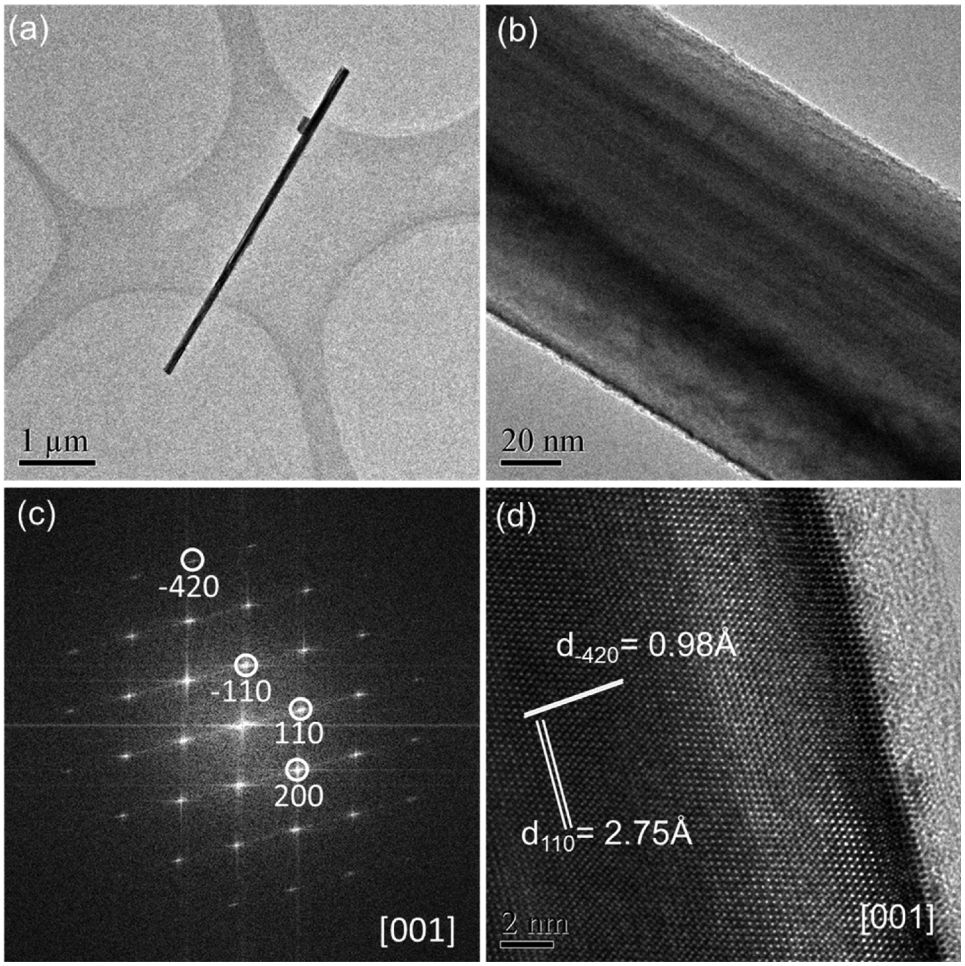

Fig. 3. High-resolution TEM images and electron diffraction pattern of CuO nanowires.

increased beyond 700 °C, the surface of electrodes was covered by a dense film of micrometer-sized particles and the nanowires were disappeared (Fig. S2). It can be clearly observed that the uniform CuO nanowires were grown in the direction essentially perpendicular to the substrate, revealing a close contact between nanowires and substrates because of its *in-situ* growth on the substrates.

We further characterized the crystalline structure of these CuO nanowires using high-resolution TEM and electron diffraction. As shown in Fig. 3, the prepared CuO nanowires exhibited well-defined fringe space patterns of a single crystal. Analysis of the corresponding electron diffraction pattern patterns clearly indicates that all the produced nanowires were single-crystalline CuO with a monoclinic crystal structure. The measured lattice spacing values of 2.75 Å and 0.98 Å are corresponding to the interplanar spacing for the (110) and (−421) planes of a pure monoclinic CuO crystal, respectively.

Together considering the results obtained from XRD, Raman and TEM characterizations, we can have a clear image about the structure of the electrodes prepared by thermal treatment using Cu foils: the outer layer is CuO nanowires in the length range of 5 to 20 μm, the inner layer is the Cu substrate which are not oxidized, and a thin layer of Cu_2O species in between. The schematic description of the structural composite for the prepared electrodes can be schematically depicted in Fig. 4. The contact between three composites are compact enough as the CuO nanowire and Cu_2O layer are *in-situ* generated on the Cu foil. The XRD characterizations of one-step and two-step photoelectrodes were also collected (Fig. 5a), from which we can see that there is no obvious discrepancy of crystalline and phase structure for one-step or two-step process. Besides, the morphologies and crystallinity of CuO nanowires give no obvious differences regardless of the one-step or two-step thermal treatment. The SEM images of the one-step and two-step photoelectrodes exhibited that the apparent contacting interface between nanowires and substrates after two-step treatment is more compactable than one-step calcination, which is due to the pre-treatment under low temperatures (Fig. 5b). The compact interface at the nanowires and substrates will be beneficial for the charge transferring from the nanowires to the substrates. To confirm the role of compact interface for charge transferring, we employed electrochemical impedance spectroscopy to characterize the samples after one-step and two-step calcinations (Fig. S3). The result shows that the a much smaller arc radius was achieved for two-step calcinations compared with one-step calcination, indicating that the charge transfer resistance is much smaller for two-step calcinated samples, which means that photogenerated charge separation is much more efficient after two-step calcination.

To evaluate the PEC water splitting activity of various photocathodes prepared under different temperatures, linear sweep photovoltammetry test was conducted under 0.2 Hz chopped illumination with an intensity of 100 mW cm^{-2} in 1.0 M Na_2SO_4buffered at a pH of 6.8, which was the electrolyte used in all the PEC experiments in this study. The PEC performance for the CuO electrodes prepared by one-step and two-step calcination under different temperatures is shown in Fig. 6, which can be used to evaluate the photoelectrochemical behaviors under the same experimental conditions. All these samples exhibit evident photocurrent responsive characters of a typical p-type semiconductor. The onset potential of these samples for water reduction initiates at about 700 mV versus RHE, which is a relatively positive

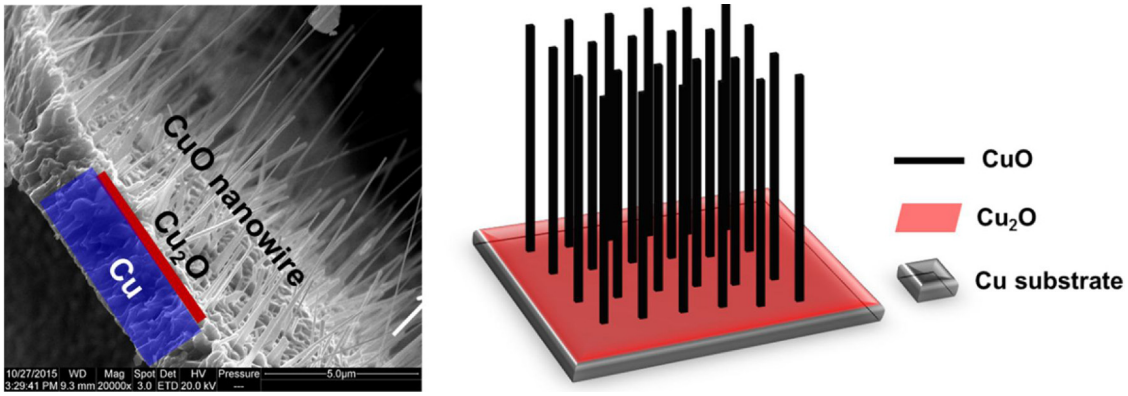

Fig. 4. Morphology and structure scheme of $Cu/Cu_2O/CuO$ photocathode prepared via thermal treatment process.

onset potential of photocathodes for PEC water splitting. As we know, a more positive onset potential of photocathodes will be more suitable to cooperate with photoanodes for constructing a no-bias PEC water splitting cell. It can be found the photocurrents of two samples prepared via two-step calcination is higher than the case of one-step under the same temperature, implying that the pre-treatment under low temperature is beneficial for an enhanced PEC activity of the electrode. Taking two samples, CuO-500 and CuO-300-500 as examples, although both samples are prepared under 500 °C, the photocurrent of CuO-300-500 is more than 20% higher than CuO-500, which may be attributed to the more compact contacting interface between CuO nanowires and the substrates after pre-treatment under 300 °C. Although the pre-treatment under low temperature (e.g., 300 °C) is not capable to generate CuO nanowires, it can induce the formation of very thin CuO layer gradually, and such layer is most possibly to functionalize as precursor for the formation of nanowires and act as protecting layer to inhibit the excessive oxidation of Cu substrates to some extent. Notably that the photocurrent of the photocathodes treated under the temperature below 400 °C or beyond 800 °C is relatively low because the lower temperature cannot induce the formation of CuO nanowires while the higher temperature can deeply oxidize the Cu foil to CuO, resulting in the poor conductivity of substrate. The superior PEC performance is achieved for the CuO-300-500 sample, exhibiting a photocurrent of $\sim 1.4\ mA\ cm^{-2}$ at 0 V vs. RHE under AM 1.5 G irradiation. As far as we know, it is one of the highest photocurrents based on bare CuO photocathode for PEC water splitting compared with some relative systems reported so far (Table S1) [17,18,23,30,31].

Fig. 7 shows the optimized performance of the bare CuO nanowire-based photocathode and the photo-stability measurement held at 0 V vs. RHE. Although the initial photocurrent of CuO electrode is high and the onset potential is positive enough, the photocurrent dramatically declines at a very short time even in a few seconds. The photocurrent was further decreased to $-0.4\ mA\ cm^{-2}$ in less than 10 min, which is only 35% of the initial photocurrent. The poor stability of CuO photocathode may be induced by the reduction of CuO to Cu_2O and Cu by photogenerated electrons, and these part of electrons is unable to participate in proton reduction for hydrogen production.

To improve the stability of CuO photoanode, a general strategy is

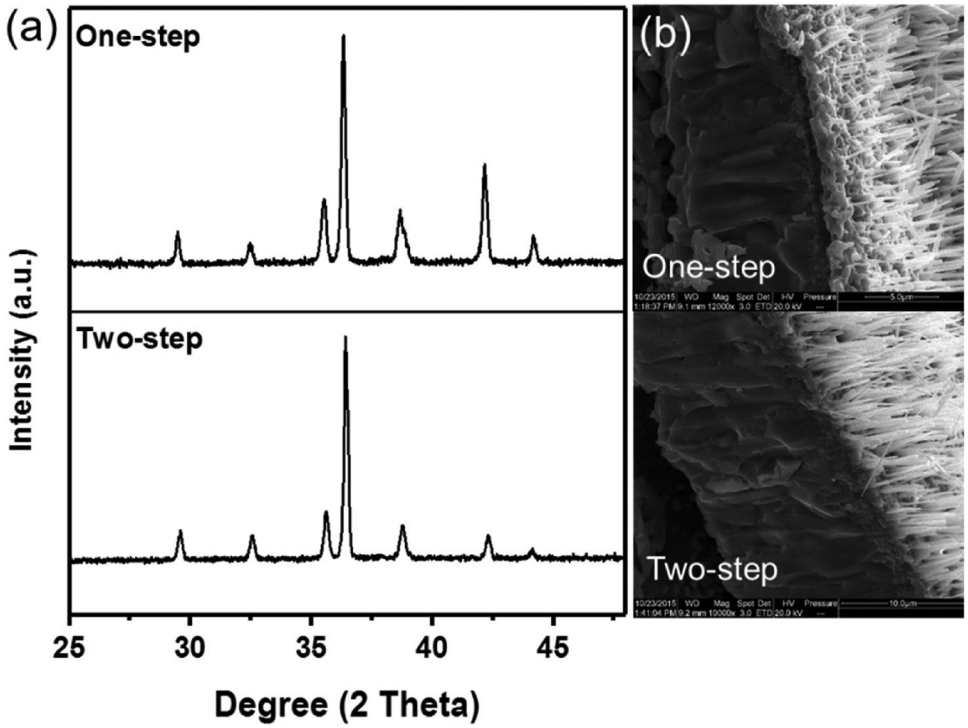

Fig. 5. XRD (a) and SEM (b) characterizations of photoelectrodes treated via one-step and two-step calcinations. The temperature was fixed to 500 °C and the pre-treated temperature for two-step calcination was 300 °C for 1 h.

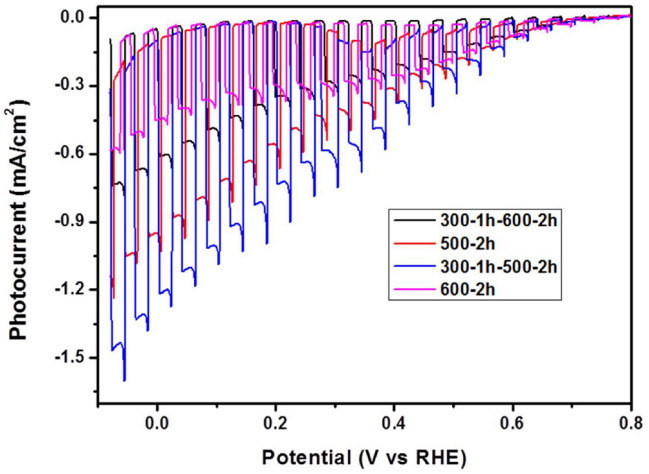

Fig. 6. Current-potential (I–V) characteristics curve of CuO photocathodes prepared by one-step and two-step processes under different temperatures. 300-1 h-600-2 h means the photocathode was prepared under 300 °C for 1 h and then treated at 600 °C for 2 h.

introducing some active sites on the surface to accelerate the reaction rate of proton reduction for quickly consuming the photogenerated electrons and meanwhile inhibit the charge accumulation on the surface. In this work, Pt was chosen as cocatalyst to deposit on the surface of CuO nanowire using an electrodeposition method in the presence of H_2PtCl_6 solution (0.01 g/L) under the applied potential of −0.5 V vs. RHE. The amount of Pt was controlled by varying the deposition time for electro-deposition. Fig. 8 shows the SEM images of CuO nanowires after depositing of Pt particles under different deposition times. It can be evidently observed that the Pt particles with size ranging from 10 to 30 nm are deposited on the surface of CuO nanowires. The size of Pt particles were further increased to more than 50 nm when the deposition time was prolonged to 300 s under the same applied potential. It is well-known that the Pt can accelerate the reaction rate of proton reduction for hydrogen production by photoexcited electrons. The amount of Pt cocatalyst was also optimized and the best PEC performance was achieved when Pt was electrodeposited for 30 s (Fig. S4). Further increasing the deposition time leads to a decline of the PEC activity. Fig. 9 shows the PEC water splitting performance of CuO nanowires with or without Pt deposition. Although the photocurrent of Pt/CuO is just slightly higher than bare CuO electrode, an obvious difference between Pt/CuO and bare CuO electrodes is the sharp photocathodic current spike while illumination was turned on and off. For bare CuO, there appears an sharp current spike while almost no spike appears after depositing Pt on the surface. When light reaches the photoelectrodes, photogenerated charges in the CuO electrodes will separate and transfer to the semiconductor/solution interface and then accumulate at the surface because of slow reaction kinetics. The slow reaction kinetics induces a sharp current spike that decays as the accumulation process perturbs the charge distribution of the space charge region until equilibrium is eventually reached between surface reactions and charge recombination [26–29]. For a p-type photocathode system as described in this work, the cathodic transient peak should be assigned to the electrons diffusing from the external circuit and recombining with the accumulated holes at the semiconductor/solution interface. After depositing Pt nanoparticles on CuO photocathode, the photogenerated electrons transferring to the CuO surface can be quickly trapped by Pt cocatalysts for participating hydrogen production reaction, resulting in the remarkable decreasing of charge accumulating at the interface between semiconductor and solution. This is the reason why the cathodic transient peaks almost disappeared after Pt nanoparticles were deposited. Electrochemical impedance results confirmed that the much more efficient charge separation and charge transferring can only be achieved after depositing Pt cocatalyst compared with the bare photoelectrode, which is most possibly attributed to the reducing charge accumulation and promote the spatial charge separation by Pt cocatalyst (Fig. S5). The photo-stability of Pt/CuO electrode is shown in Fig. 9b, showing that the photocurrent of Pt/CuO at 0 V vs. RHE can be maintained to more than 80% of its initial value after illumination for more than 10 min, implying that the photo-stability of Pt/CuO photoelectrode is greatly improved compared with bare CuO in Fig. 7. The hydrogen gas was indeed produced during the PEC evaluation for Pt/CuO photoelotrode under the illumination of 300 W Xe lamp. (Fig. S6) Because the photo-stability of CuO photocathode is not very good, the gas evolution declined quickly after reaction for 20 min. For potential utilization of this photocathode for an integrated no-bias PEC system, the photocurrent and the photo-stability of CuO photoelectrode require to be further improved in the future work.

4. Conclusion

In summary, one-dimensional CuO nanowires was successfully fabricated on Cu foils as photocathode via a facile thermal treatment process. The well-defined CuO nanowire-based photocathodes exhibit an obvious photocurrent responsive character of a p-type semiconductor with a positive onset potential of ~700 mV vs. RHE. The CuO photocathode shows a photocurrent of ~1.4 mA cm^{-2} at 0 V vs. RHE under AM 1.5 G irradiation, which is one of the highest

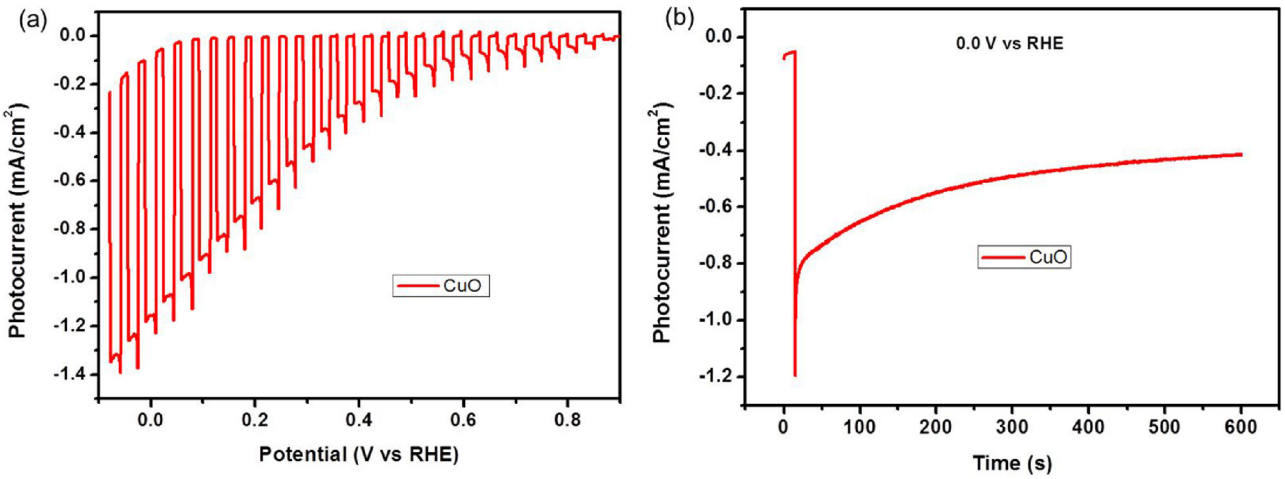

Fig. 7. Current-potential (I–V) characteristics curve and stability test of CuO photocathode for PEC water splitting. The CuO-300-1 h-500-2 h photocathode was used in the I–V and stability test.

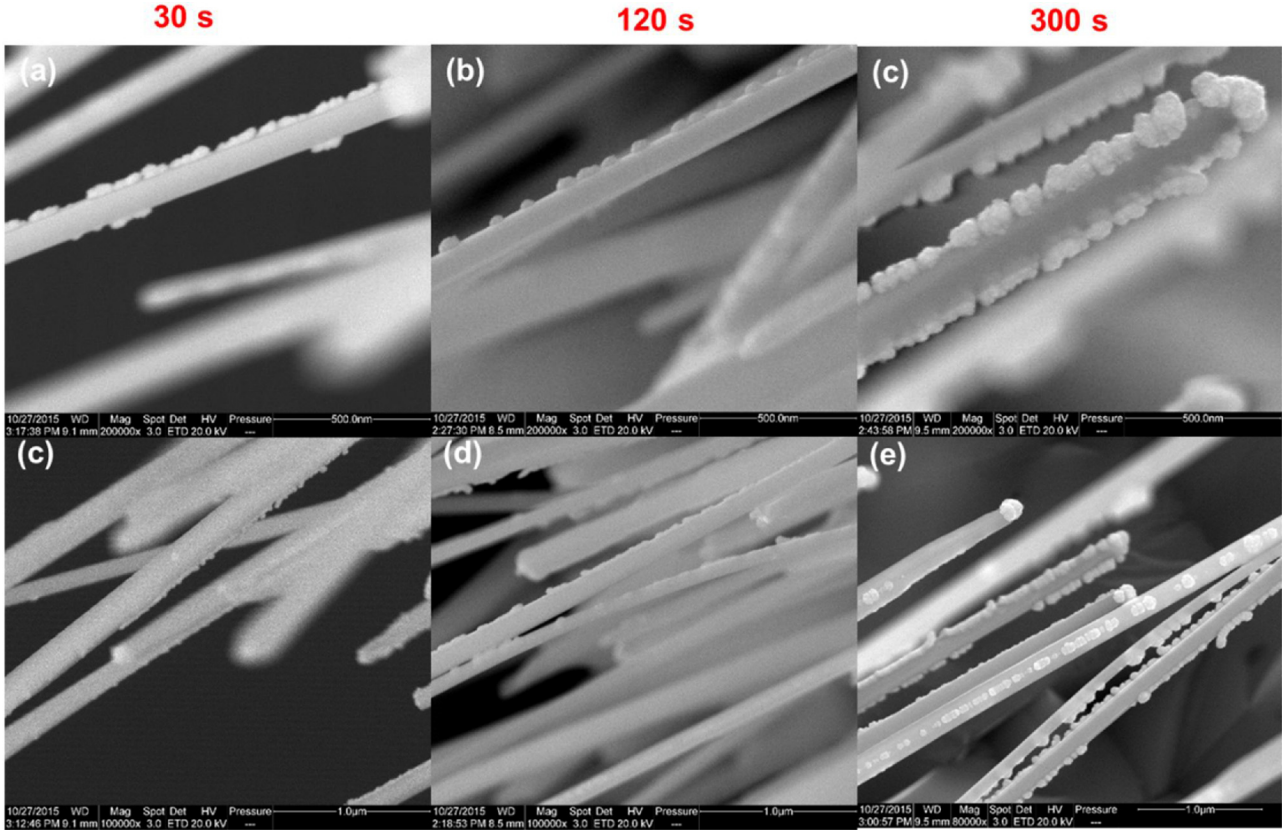

Fig. 8. SEM images of CuO nanowire after depositing Pt particles using electro-deposition method under different deposition time. (a, c) 30 s; (b, d) 120 s and (c, e) 300 s. Pt cocatalyst was deposited in a three-electrode system, the applied bias is −0.5 V.

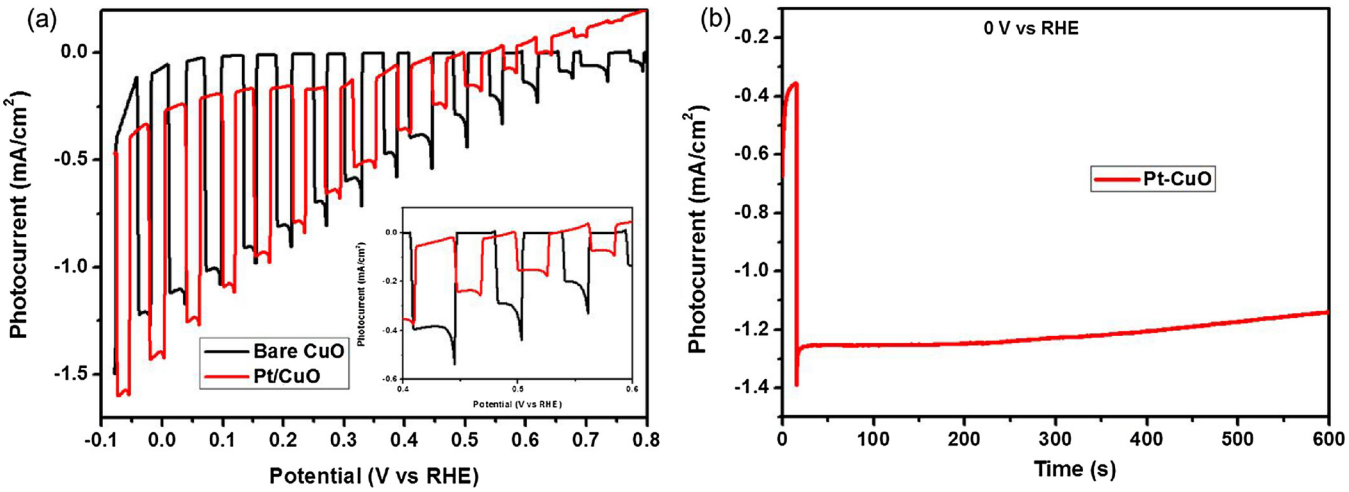

Fig. 9. Current-potential (I–V) characteristics curve (a) and photo-stability (b) of CuO photocathodes after deposition of Pt particles as cocatalysts.

photocurrents based on bare CuO photocathode for PEC water splitting. Further depositing Pt nanoparticles as cocatalyst on the surface of CuO nanowires to accelerate surface reaction and inhibit charge accumulating at semiconductor/solution interface, resulting in a significant improvement of the stability for photoelectrodes. Our work reports a simple and promising method for fabricating well-defined metal oxides-based photoelectrodes, which providing a promising candidate for highly efficient no bias PEC devices for solar fuels production.

Acknowledgements

This work is financially supported by National Natural Science Foundation of China (21501236, 21673230), Dalian Institute of Chemical Physics (DICP ZZBS201610), Youth Innovation Promotion Association of Chinese Academy of Sciences (2016167) and the R&D department of PetroChina. The authors would like to thank Prof. Mingrun Li at DICP for HRTEM characterization.

Appendix A. Supplementary data

Supplementary material related to this article can be found, in the online version, at doi:https://doi.org/10.1016/j.apcatb.2018.08.070.

References

[1] S. Perathoner, G. Centi, D.S. Su, ChemSusChem 9 (2016) 345–357.
[2] G. Knor, Coord. Chem. Rev. 304 (2015) 102–108.
[3] J.C. Colmenares, R. Luque, Chem. Soc. Rev. 43 (2014) 765–778.
[4] Y.Q. Qu, X.F. Duan, Chem. Soc. Rev. 42 (2013) 2568–2580.
[5] T. Hisatomi, J. Kubota, K. Domen, Chem. Soc. Rev. 43 (2014) 7520–7535.
[6] S.Y. Reece, J.A. Hamel, K. Sung, T.D. Jarvi, A.J. Esswein, J.J.H. Pijpers, D.G. Nocera, Science 334 (2011) 645–648.
[7] K.S. Joya, Y.F. Joya, K. Ocakoglu, R. van de Krol, Angew. Chem. Int. Ed. 52 (2013) 10426–10437.
[8] S.S. Zhang, J. Yan, S.Y. Yang, Y.H. Xu, X. Cai, X. Li, X.C. Zhang, F. Peng, Y.P. Fang, Chin. J. Catal. 38 (2017) 365–371.
[9] R.G. Li, Chin. J. Catal. 38 (2017) 5–12.
[10] A. Paracchino, V. Laporte, K. Sivula, M. Gratzel, E. Thimsen, Nat. Mater. 10 (2011) 456–461.
[11] Q. Huang, Z. Ye, X.D. Xiao, J. Mater. Chem. A Mater. Energy Sustain. 3 (2015) 15824–15837.
[12] O. Khaselev, J.A. Turner, Science 280 (1998) 425–427.
[13] P.P. Sahoo, B. Zoellner, P.A. Maggard, J. Mater. Chem. A Mater. Energy Sustain. 3 (2015) 4501–4509.
[14] P.R. Shao, S.Z. Deng, J. Chen, J.A. Chen, N.S. Xu, J. Appl. Phys. 109 (2011) 023710.
[15] Y.K. Jeong, G.M. Choi, J. Phys. Chem. Solids 57 (1996) 81–84.
[16] C.Y. Chiang, K. Aroh, S.H. Ehrman, Int. J. Hydrogen Energy 37 (2012) 4871–4879.
[17] C.Y. Chiang, K. Aroh, N. Franson, V.R. Satsangi, S. Dass, S. Ehrman, Int. J. Hydrogen Energy 36 (2011) 15519–15526.
[18] J.F. Han, X. Zong, X. Zhou, C. Li, RSC Adv. 5 (2015) 10790–10794.
[19] X.C. Jiang, T. Herricks, Y.N. Xia, Nano Lett. 2 (2002) 1333–1338.
[20] S.L. Cheng, M.F. Chen, Nanoscale Res. Lett. 7 (2012) 119.
[21] C.W. Li, M.W. Kanan, J. Am. Chem. Soc. 134 (2012) 7231–7234.
[22] O.M. Auslaender, H. Steinberg, A. Yacoby, Y. Tserkovnyak, B.I. Halperin, K.W. Baldwin, L.N. Pfeiffer, K.W. West, Science 308 (2005) 88–92.
[23] Z.H. Zhang, P. Wang, J. Mater. Chem. 22 (2012) 2456–2464.
[24] W.Z. Wang, O.K. Varghese, C.M. Ruan, M. Paulose, C.A. Grimes, J. Mater. Res. 18 (2003) 2756–2759.
[25] Y. Chang, J.J. Teo, H.C. Zeng, Langmuir 21 (2005) 1074–1079.
[26] F. Le Formal, N. Tetreault, M. Cornuz, T. Moehl, M. Gratzel, K. Sivula, Chem. Sci. 2 (2011) 737–743.
[27] F. Le Formal, M. Gratzel, K. Sivula, Adv. Funct. Mater. 20 (2010) 1099–1107.
[28] P. Iwanski, J.S. Curran, W. Gissler, R. Memming, J. Electrochem. Soc. 128 (1981) 2128–2133.
[29] M.G. Walter, E.L. Warren, J.R. McKone, S.W. Boettcher, Q.X. Mi, E.A. Santori, N.S. Lewis, Chem. Rev. 110 (2010) 6446–6473.
[30] A. Paracchino, J.C. Brauer, J.E. Moser, E. Thimsen, M. Graetzel, J. Phys. Chem. C 116 (13) (2012) 7341–7350.
[31] S.M. Panah, R.S. Moakhar, C.S. Chua, H.R. Tan, T.I. Wong, D.Z. Chi, G.K. Dalapati, ACS Appl. Mater. Interfaces 8 (2) (2016) 1206–1213.